Fermilab Library
0 1160 0031347 2

CSR-93-16

Massachusetts Institute of Technology

ASTROPHYSICS

Submitted to *The Astrophysical Journal*
August 3, 1993

FORMATION AND EVOLUTION OF LUMINOUS SUPERSOFT X-RAY SOURCES

S. Rappaport[1], R. Di Stefano[1,2,3] and J.D. Smith[1]

MIT, LNS

T

Preprint Series No. CSR-93-16

FERMILAB
SEP 27 1993
LIBRARY

[1]Department of Physics, Massachusetts Institute of Technology, Cambridge, Massachusetts 02139

[2]*Address after September 1, 1993*: Harvard-Smithsonian Center for Astrophysics, 60 Garden Street, Cambridge, MA 02138

[3]On leave from the Department of Physics, New York Institute of Technology, Old Westbury, NY 11568

Department of Physics
Department of Mathematics
Department of Earth, Atmospheric, and Planetary Sciences
Center for Space Research
Center for Theoretical Physics
Research Laboratory of Electronics

57-42

Abstract

Luminous supersoft X-ray sources, with characteristic luminosities of ~10^{38} erg s^{-1} and temperatures, kT, of ~35 eV have been established as a new and distinct class of X-ray source through recent Rosat observations. Several possible physical models have been proposed for these sources. One promising scenario (van den Heuvel et al. 1992) involves mass transfer, which is unstable on a thermal time scale, from a main-sequence or subgiant donor star onto the surface of a white dwarf. For a narrow range of accretion rates, steady nuclear burning of the accreted matter can take place. This process can provide the high luminosities and the correct range of temperatures observed in the supersoft sources. However, given the limited range of mass transfer rates that are consistent with this phenomenon, it is far from obvious that a sufficient population of such systems exists in galaxies such as our own, M31, and the Magellanic clouds, in order to account for the large number of supersoft sources which can be inferred from present observations. This work addresses the population question in detail, through a Monte Carlo simulation of the formation and evolution of such systems, which starts with zero-age primordial binaries. In order to evolve into close binary systems which contain a white dwarf component and a companion transferring mass at a rate within the requisite narrow range, a binary system must undergo a specific progression of evolutionary steps. We find that a sufficient subset of our initial binaries evolve to become systems with the requisite properties, so that they can account for the population of supersoft sources that is inferred from observations. In particular, we find that there should be more than 1000 systems in the Galaxy today with properties that very closely match those of the observed supersoft sources. From our models, we find expected luminosities, white dwarf effective temperatures, and orbital periods in the ranges of $10^{37} - 10^{38}$ ergs s^{-1}, $(1 - 5) \times 10^5$ K, and 8 hours – 1.4 days, respectively. The masses of the white dwarf and donor star are expected to lie in the range of $0.7 - 1.05\ M_\odot$ and $1.3 - 2.7\ M_\odot$.

1. Introduction

Luminous supersoft X-ray sources were originally discovered during a survey of the Large Magellanic Cloud with the Einstein Observatory (Long et al. 1981) and have now been established as a new and distinct class of luminous X-ray binary by the recent Rosat all-sky X-ray survey (Truemper et al. 1991; Greiner, Hasinger, & Kahabka 1991; Schaeidt, Hasinger, & Truemper 1993; Orio & Ogelman 1993; Hertz, Grindlay, & Bailyn 1993). They have characteristic luminosities of up to $\sim 10^{38}$ ergs s^{-1} and effective temperatures of $\sim 4 \times 10^5$ K (kT $\simeq$ 35 eV). The known supersoft sources include 5 in the LMC, 4 in the SMC, 2 in our Galaxy, 8 in M31, 1 in NGC 253, and 1 in M101 (Truemper 1993, private communication). The characteristic photon energies in the supersoft X-ray sources are about a factor of 100 times lower than for more conventional X-ray binaries. Because the very soft X-rays are readily absorbed after only a relatively short path through the interstellar medium, even if there is a significant population of these sources, most of them would be difficult to detect.

The two supersoft sources that were discovered with Einstein, CAL 83 and CAL 87 (Long et al. 1981), have been identified with optical counterparts in the LMC. CAL 83 has V ~ 17 and an orbital period of 1.04 days (Smale *et al.* 1988; Pakull *et al.* 1988), while CAL 87 has V ~19 and an orbital period of 10.6 hours (Naylor *et al.* 1989; Callanan *et al.* 1989; Cowley et al. 1990). The optical companion stars in CAL 83 and CAL 87 have been estimated to have masses in the range of $1.5 - 2\ M_\odot$. Given orbital periods of ~0.5 – 1 day, the companion stars cannot have evolved very far from the main sequence.

There have been suggestions that these supersoft X-ray sources are binary systems containing black holes (see, e.g., Cowley et al. 1990) or neutron stars (see, e.g., Greiner et al. 1991; Kylafis & Xilouris 1993) that are accreting near to or above the Eddington limit. In this scenario, the emerging radiation interacts with surrounding matter and is thereby downgraded in energy. Because such soft X-rays are easily absorbed by the interstellar medium, there has been speculation that many of the low-mass X-ray binaries (LMXBs) could spend a significant fraction of their time in a "supersoft" state, thereby rendering them substantially less detectable. If this were indeed the case, it might contribute to an understanding of the apparent lack of sufficient LMXBs to serve as the putative progenitors of recycled millisecond pulsars (Kulkarni & Narayan 1988). These are attractive propositions, but for a number of reasons we believe that it is worthwhile to explore the possibility that the correct model for these sources lies elsewhere. For example, there is no known case of a conventional X-ray source (emitting in the 1-10 keV range) that becomes a supersoft source when the accretion rate approaches and grows beyond the Eddington limit. However, a number of counter-examples exist. They

include: (i) Very large flares in LMC X-4 which apparently exceed the Eddington limit by at least a factor of 10, while the characteristic X-ray energy decreases by at most a factor of a few (Levine et al. 1991). (ii) Transient sources with candidate black-hole accretors (see, e.g., Doxsey et al. 1976; Sunyaev et al. 1992; Casares, Charles, & Naylor 1992; van Paradijs & McClintock 1993), which also appear to approach if not significantly exceed the Eddington limit, and which can have soft spectra with kT of the order of ~1 keV, still far harder that the characteristic energies of the supersoft sources. (iii) Cen X-3, believed to be a neutron star accreting close to the Eddington limit becomes progressively harder with increasing accretion rate, until the X-rays are completely quenched at mass accretion rates above the Eddington rate (Giacconi 1975).

The particular model for these systems that we investigate in detail in the present work invokes steady nuclear burning of accreted matter on the surface of a ~ 1 $M_\odot$ white dwarf from a more massive main-sequence or subgiant companion star (van den Heuvel et al. 1992). Mass transfer rates of between 1 and 4×10^{-7} $M_\odot$ yr^{-1} are required to sustain the observed luminosities. Such high transfer rates are a natural consequence of unstable mass transfer via Roche lobe overflow in this type of system. The transfer tends to be unstable because the donor star is more massive than the accreting white dwarf; however, the rate of transfer is limited by the thermal time scale of the main-sequence donor star (Paczynski 1971; Webbink 1979; Savonije 1983; Pylyser & Savonije 1988, 1989). The masses and evolutionary states of the donor stars in the CAL 83 and CAL 87 systems are consistent with this scenario.

In this work we carry out extensive simulations of the formation and subsequent evolution of systems that may lead to supersoft sources. The aim is to explore the hypotheses that the type of system described above (i) can explain the observed properties (luminosity, temperature, orbital period) of supersoft sources, and (ii) that they can be formed in sufficiently large quantities to account for the observed numbers of such sources. Our approach, which utilizes Monte Carlo techniques, is to start with a large pool of primordial binaries and follow their evolution to determine what fraction of them end up with the requisite properties of supersoft X-ray sources. From these calculations we determine how many of these sources there should be at the current epoch in the Galaxy, in the Magellanic Clouds, and in M31. Moreover, the calculations yield a set of testable predictions about the properties of the supersoft sources.

On general grounds, we expect binaries in which mass is being unstably transferred onto a white dwarf to form, whether or not they turn out to account for the observed supersoft sources. The present study of their formation and evolution tells us what the population of such systems should be at the present epoch, and what range of observational properties they

should exhibit. As a minimum, therefore, we can make predictions of an as-yet-unobserved phenomenon.

2. The Formation and Evolution of Supersoft Systems

We have developed a Monte Carlo code to study the formation and evolution of supersoft systems, modeled as binaries in which matter is accreting unstably onto a white dwarf on a time scale governed by the thermal time scale of the donor star (van den Heuvel et al. 1992). Basically, we start with a very large number (e.g., 3×10^6) of primordial binaries with primary stars in the correct range to produce massive white dwarfs. We then follow these systems through their various evolutionary phases to see how many end up forming systems that we consider to be good candidates for supersoft systems.

Briefly, we believe that the evolutionary path to a successful supersoft system consists of the following basic elements: (1) a primordial binary with a primary whose mass, M_p, is in the range of $1.8 \sim 8\ M_\odot$ and a secondary of mass, M_s, greater than $\sim 0.8\ M_\odot$; (2) an episode of unstable mass transfer from the primary during which a common envelope forms and the secondary spirals in toward the core of the primary; (3) an end product of the common envelope phase which is a close binary consisting of the original secondary in orbit with a less massive white dwarf (the core of the primary); (4) an era of unstable mass transfer onto the white dwarf which takes place on the thermal time scale of the secondary; and finally (5) a mass transfer rate within the narrow range consistent with steady nuclear burning.

At first glance, it might seem highly improbable that this sequence of events would occur. In fact, we show below that there should be nearly one thousand such systems in the Galaxy at any given epoch. We discuss below the steps used in the code to study the formation and evolution of these systems.

2.1 Generating the Progenitor Binary System

We use Monte Carlo techniques to generate the initial binary system. The primary mass is chosen from Eggleton's (1993) Monte Carlo representation of the Miller & Scalo (1979) initial mass function (IMF):

$$M(x) = \frac{0.19\,x}{(1-x)^{0.75} + 0.032\,(1-x)^{0.25}} \tag{1}$$

where x is a uniformly distributed pseudo-random number. Next, the mass of the secondary, M_s, is chosen from one of several probability distributions, f(q), of mass ratio (see, e.g., Abt

& Levy 1976, 1978, 1985; Abt, Gomez, & Levy 1990; Tout 1991; Duquennoy & Mayor 1991), where $q \equiv M_s/M_p$. We have tested a simple distribution that is uniform in q, as well as an uncorrelated distribution where the secondary mass is chosen from the same IMF as was the primary mass (see, e.g., Duquennoy & Mayor 1991, hereafter DM, for a related discussion). In addition, we studied another distribution in q which rises toward lower mass secondaries and reaches a peak at q = 0.23 (DM). We note, however, that for more massive stars in binaries there seems to be compelling evidence for a substantial correlation between masses (Garmany, Conti, & Massey 1980). For our "Standard Model" we somewhat arbitrarily adopt $f(q) \propto q^{1/4}$ (Abt & Levy 1978).

Finally, an orbital period is chosen. In our standard model, we choose from a distribution that is uniform in log(P) over the period range 0.5 days to 10^6 years. We also consider other plausible distributions of P, including a Gaussian shape in log(P) centered at P = 180 years (see, e.g., Abt & Levy 1978; Duquennoy & Mayor 1991). After the masses and orbital period are picked, the orbital separation is calculated from Kepler's law.

A series of tests is used to eliminate systems that cannot evolve into candidates for supersoft X-ray sources. For example, if one of the stars initially overfills its Roche lobe (i.e., R_p greater than the Roche lobe radius R_L), then we drop the system from the simulation. We also drop systems in which the secondary has a mass of less than 0.8 $M_\odot$. The reason for this is two-fold. First, if such a star should eventually overfill its Roche lobe, it would likely be transferring mass to a white dwarf that is only marginally less massive, and so there would not be an extended era of unstable mass transfer. Moreover, the thermal time scale would be sufficiently long that the rate of mass transfer would be much smaller than is required. We also drop systems in which R_L is greater than the maximum radius of a giant of that mass (i.e., there would be no Roche-lobe overflow). Table 1 lists the percentages of systems surviving these and other "cuts" that are made at various stages of the evolution to identify potential supersoft sources (see §2.1).

Having generated a set of viable binary systems via Monte Carlo techniques, each of which has the potential to evolve to a system in which a white dwarf is accreting mass in an unstable mass transfer process, we now proceed analytically. We utilize an analytic expression for the relation among the core mass, the radius, and the total mass of the primary to estimate the mass of the degenerate core, M_{WD}, when the primary fills its Roche lobe. An analytic expression for this purpose was designed to reproduce the features of Figure III.2 of Politano (1988) and Figure 1 of de Kool (1992), except that the core-mass radius relation for stars near 1 $M_\odot$ was renormalized to match the fitting formula of Eggleton (see eq. 4 of Joss, Rappaport, & Lewis 1987). No account was taken of wind mass loss in the AGB phase before mass transfer

commences.

2.2 The Route to Thermally Unstable Mass Transfer

The era of interest to this work is a possible extended period of unstable mass transfer, on a thermal time scale, from the secondary to a white dwarf, which is the compact remnant of the primary star. In order for the system to reach this stage, a common envelope phase (see e.g., Webbink 1992, and references therein) must occur in order to (i) eject the envelope of the primary and "uncover" its degenerate core, and (ii) to transform the initially wide orbital system to a more compact binary. Finally, some mechanism (e.g., magnetic braking or nuclear evolution) must bring the secondary to fill its Roche lobe in order to initiate unstable mass transfer onto the white dwarf.

In order to select only systems which undergo a common envelope phase we require that the radius of the Roche lobe of the primary be larger than the radius of a star of mass M_p at the base of the asymptotic giant branch (AGB; see, e.g., Paczynski 1965; Webbink 1979, 1985, 1992, de Kool 1992, and references therein). This ensures that unstable mass transfer will occur on a time scale that is much shorter than a thermal time, and should lead to a common envelope phase. We proceed to derive the properties of the system at the end of this phase, namely the mass of the white dwarf and the orbital separation.

Once mass transfer commences, we assume that a common envelope phase occurs and compute the final spiral-in separation from simple energetic considerations (see, e.g., Sparks & Stecher 1974; Paczynski 1976; Taam, Bodenheimer, & Ostriker 1978; Meyer & Meyer-Hofmeister 1979; Livio & Soker 1988; Webbink 1992). The expression we use for determining a_f, the final orbital separation after spiral-in, is given by:

$$\frac{\varepsilon\, GM_s}{2}\left[\frac{M_{core}}{a_f} - \frac{M_p}{a_i}\right] = \frac{GM_{env}(M_{env} + 3M_{core})}{R_p} \quad , \qquad (2)$$

where M_{core} and M_{env} are the core and envelope masses of the primary, R_p is the radius of the primary, a_i is the initial orbital separation, and ε is the energy efficiency factor for ejecting the envelope. We take ε to have a value of 0.3 in our standard model. The two terms in parentheses on the right hand side of equation (2) represent the binding energy of the envelope of the primary to itself and to its core. The dimensionless coefficients multiplying each term were computed for an assumed polytropic envelope structure with polytropic index n = 3.5. For other values of n the ratio of ~3:1 between the two coefficients is roughly the same. We assume that the duration of the spiral-in is sufficiently short (~10^4 yr; see above references) that the mass of the secondary does not change significantly during the common envelope phase.

After the spiral-in episode, the separation, the white dwarf mass, the secondary mass, and the corresponding Roche-lobe radius of the secondary are known. If the secondary is less massive than the white dwarf, we eliminate the system from further consideration, since any subsequent mass transfer is likely to be stable.

If at the end of the common envelope phase the secondary is already overfilling its Roche lobe, then we eliminate the system. (In most cases, this circumstance would be expected to lead to a merger of the secondary star with the degenerate core with the primary, which presumably would result in the formation of a giant star.) If the Roche lobe is so large that in order to fill it the secondary would have to evolve past the base of the giant branch, then we also eliminate the system, since mass transfer would then be dynamically unstable rather than unstable on a thermal time scale (see, e.g., Paczynski 1967; Kippenhahn, Kohl, & Weigert 1967; Webbink 1979, 1992).

All of the systems that remain, roughly 3% of the systems we started with, will experience mass transfer from the secondary to the white dwarf which is unstable on a thermal time scale, and hence are potential candidates for supersoft X-ray sources.

2.3 Nuclear Burning

The observable characteristics of each of the supersoft candidates depends critically upon the rate of mass transfer, which determines whether matter accreted onto the surface of the white dwarf will be able to be burned in a steady manner. The mass transfer rate onto the white dwarf is computed from the simple expression

$$\dot{M} = 0.5 \times \{M_s(0) - M_{WD}(0)\}/\tau_{KH}, \tag{3}$$

where τ_{KH} is the Kelvin time scale of the secondary, and $M_s(0)$ and $M_{WD}(0)$ are the masses of the secondary star and the white dwarf (the core of the original primary) immediately after the common envelope phase. Realistically, the mass transfer rate is more likely to change with time than to have the constant value given by equation (3). However, it is beyond the scope of this paper to model the unstable mass transfer process in detail.

For each white dwarf mass, we define $\dot{M}_{crit}$ as the *maximum* rate at which steady, stable nuclear burning on the surface of a white dwarf can consume the accreted matter without the star puffing up to become a red giant. A convenient fitting formula for $\dot{M}_{crit}$ is:

$$\dot{M}_{crit} \simeq 8 \times 10^{-7} (M_{WD} - 0.5) \quad M_\odot \, yr^{-1} \ , \tag{4}$$

for the case in which the accreted matter is of solar composition and where M_{WD} is expressed in units of $M_\odot$ (Paczynski 1970a,b; Uus 1970; Iben 1982). An expression for the *minimum* rate of mass transfer compatible with steady nuclear burning is given by

$$\dot{M}_{stable} \simeq 1.32 \times 10^{-7} (M_{WD})^{3.59} \quad M_\odot \, yr^{-1} \ , \tag{5}$$

(Iben 1982). If the mass transfer rate $\dot{M}$ is less than $\dot{M}_{stable}$, then detailed calculations indicate that nuclear burning will be unstable and the nuclear luminosity will be generated only episodically as nova outbursts (for very small values of $\dot{M}$) or as part of limit cycle without substantial hydrodynamic mass loss (Paczynski & Zytkow 1978; Sion, Acierno, & Tomczyk 1979; Nomoto, Nariai, & Sugimoto 1979; Sienkiewicz 1980; Taam 1980a,b; Kutter & Sparks 1981; Prialnik et al. 1982; Nomoto 1982; Iben 1982; Sion & Starrfield 1986, 1993; Livio, Prialnik, & Regev 1989).

In order to be counted as a supersoft system immediately after the onset of mass transfer, we require that $\dot{M}_{stable}(0) < \dot{M} < \dot{M}_{crit}(0)$. Even for systems which satisfy this test, we see from equations (4) and (5) that both $\dot{M}_{crit}$ and $\dot{M}_{stable}$ depend on M_{WD}, which changes with time if there is steady nuclear burning taking place on the white dwarf (i.e., if the accreted mass is retained). In this case $\dot{M}_{stable}$ may grow to exceed $\dot{M}$, which in these calculations we have taken to be constant in time, and therefore the nuclear burning could become unstable at some point. In the case where $\dot{M}$ varies with time (e.g., an exponential decay) the same basic issue arises.

We have therefore calculated two sets of results. In the first, we show the properties of the simulated systems which have values of $\dot{M}$ within the stability limits set by $\dot{M}_{crit}(0)$ and $\dot{M}_{stable}(0)$ just after the onset of mass transfer to the white dwarf. In the second set, the properties of a given system are those found at a uniformly chosen random time, $\mathbf{t}$, during the mass transfer phase (i.e., for a random fraction of τ_{KH}). These latter results are more closely related to what an astronomer would be likely to observe. Moreover, to be conservative, we require that, in order for a source to be observable as a supersoft source at the present epoch, the value of $\dot{M}$ given by equation (3) must currently be within the range $\dot{M}_{stable}(\mathbf{t}) < \dot{M} < \dot{M}_{crit}(\mathbf{t})$ (as well as to be within this range at the start of mass transfer).

For the amount of mass, ΔM, transferred from the secondary to the white dwarf by the present time, we take

$$\Delta M = \dot{M} \, \mathbf{t} \tag{6}$$

where $\mathbf{t}$ is described above. For the simulations of supersoft sources and their properties at the

current epoch, we take the masses of the secondary and the white dwarf to be $\{M_s(0) - \Delta M\}$ and $\{M_{WD}(0) + \Delta M\}$, respectively. The orbital period is taken to decrease by an amount given by conservation of orbital angular momentum. If the mass of the white dwarf exceeds the Chandrasekhar limit, the system is recorded in the pool of potential type-Ia supernovae, but is not counted as a supersoft source. (We return to the issue of type-Ia supernovae below.)

The details of non-steady nuclear burning cycles when $\dot{M} < \dot{M}_{stable}$ (equation [5]) depend on the mass of the white dwarf, the accretion rate, and the thermal history of the white dwarf. To be on the conservative side we simply eliminated systems with $\dot{M} < \dot{M}_{stable}$, even though it seems reasonable to suppose that a substantial fraction of them will, at times, have properties that closely resemble those of the supersoft systems (see, e.g., Iben 1982; Sion & Starrfield 1993). Calculations of the properties and populations of such systems should be a worthwhile undertaking for future studies.

While we have also eliminated systems with $\dot{M} > \dot{M}_{crit}$ from our simulations, it is possible that they may also produce some sort of nuclear burning limit-cycle which yields properties similar to those of supersoft sources during certain intervals of time (see van den Heuvel et al. 1992). In particular, at least in the case of spherical accretion, one would expect the atmosphere of a white dwarf accreting at $\dot{M} > \dot{M}_{crit}$ to swell up toward becoming a red giant (see, e.g., Livio et al. 1989). However, because of the finite size of the Roche lobe, which is of the order of a few solar radii in the supersoft systems we are considering, the expansion of the atmosphere of the white dwarf is necessarily limited. Presumably, any matter extending beyond the Roche lobe will be lost from the binary system. Some future studies of nuclear burning on the surface of white dwarfs might profitably be directed toward understanding possible episodic expansions of the white dwarf atmosphere past its Roche lobe when $\dot{M} > \dot{M}_{crit}$.

Finally with regard to the issue of steady nuclear burning, we note that accretion which occurs in the type of supersoft system considered in this work would almost certainly be mediated by an accretion disk. Virtually all of the theoretical studies of nuclear burning on the surface of white dwarfs that are cited above were carried out under the assumption of spherically symmetric accretion. In order for these calculations to be relevant to the type of sources discussed here, one must assume that matter deposited at the equator of the white dwarf's atmosphere will flow around the surface of the dwarf on a time scale that is shorter than the nuclear-burning-cycle time under consideration. Moreover, the equatorial accretion must not significantly disturb the overall structure of the atmosphere of the white dwarf. On the other hand, disk accretion does have at least one advantage in terms of producing supersoft X-ray sources: the inflowing matter in the disk occupies only a relatively small solid angle, as

seen from the white dwarf, whereas the X radiation is free to propagate out from most of the surface area without substantial attenuation from the accreting material.

If the mass transfer rate is within the narrow (factor of ~3) band required for steady (or quasi-steady) nuclear burning (see references above and equations [4] and [5]), then the nuclear burning luminosity is given by

$$L_{nuc} \simeq 7.6 \times 10^{10} \left[\frac{\dot{M}}{M_{\odot}\ yr^{-1}} \right] L_{\odot} \quad , \tag{7}$$

(see, e.g., Iben 1982). In this work we consider only the nuclear burning luminosity, neglecting the accretion luminosity which contributes a relatively small fraction of the total power.

Other input parameters to the model are as follows. We take the rate of formation of primary stars in the mass range $1.8 - 8\ M_{\odot}$ to be $0.3\ yr^{-1}$. This rate was derived from the constant birthrate model of Miller & Scalo (1979; which provided a rate per unit area of the Galactic disk) and an assumed Galactic disk area of $\pi \times (12\ kpc)^2$. For simplicity, we assume that 50% of all primary stars that we choose in this mass range have binary companions. The radius of main-sequence stars, the radius of stars at the base of giant branch, and the maximum radius for any given total mass M are taken from Figure III.2 of Politano (1988).

3. Results

3.1 Profile of "Successful" Systems

In order to describe the properties of the systems that we simulate, we present two types of results. In the first, we show plots of luminosity vs. four parameters: M_{WD}, M_s, P_{orb}, and T (the latter parameter is the effective white dwarf temperature). These plots are generated for simulated systems that have just commenced mass transfer and are undergoing stable nuclear burning, as well as for those systems still undergoing stable nuclear burning at the current epoch. In these plots, each such system is represented by a single "dot", regardless of its lifetime. For the second type of result we show distributions of M_{WD}, M_s, P_{orb}, and T that are normalized so as to reflect the total number of systems expected at the current epoch.

Illustrative results of the first type for the Standard Model with luminosity vs. M_{WD}, M_s, P_{orb}, and T are shown in Figure 1 for systems just commencing mass transfer and undergoing stable nuclear burning. An analogous set of plots for systems observable at the current epoch, is shown in Figure 2. To produce Figures 1 and 2, we followed the histories of 1×10^6 and 3

$\times 10^6$ primordial binaries, respectively. At this point in the simulation, no account was taken of the lifetime of these sources; i.e., each dot in Figures 1 and 2 represents a single system. The number of binaries used to generate these plots was simply chosen so as to develop a dot pattern of the desired density.

In all four panels of Figures 1 and 2, the regions of parameter space occupied by the model supersoft systems are fairly well defined; luminosities span the range of 10^{37} to 10^{38} ergs s^{-1}. Figure 1a shows that the white dwarf in these systems typically has a mass in the range of ~0.66 to 1.05 $M_\odot$. In Figure 2a one can see how the masses of the white dwarfs have grown due to mass accretion. These figures (1a and 2a) also directly indicate how the range of luminosities depends on the white dwarf mass, as described by equations (4) and (5). The dependence of the luminosity on the mass of the secondary is shown in Figures 1b and 2b, with typical supersoft systems having secondary masses in the range of ~1.5 – 3 $M_\odot$. The explanation for the strong positive correlation between the mass of the donor star and the luminosity is that the mass transfer rate is governed primarily by the inverse of the Kelvin time of the donor star (see eq. [3]) which, in turn, varies approximately as M_s^{-3}. From Figures 1c and 2c, we find that the orbital periods of the supersoft systems should lie in the range (7 – 10) hours up to ~3 days, in very good agreement with the observations. The two numbers in parentheses describing the lower limit are for the current epoch and for systems at the onset of mass transfer, respectively. For a more detailed study of the expected orbital period distribution, which takes the lifetimes of the systems into account, see the discussion below.

In Figures 1d and 2d we display the expected luminosity vs. effective temperature of the white dwarf in supersoft systems. For a given white dwarf mass and accretion rate (or equivalently, the luminosity) we computed the effective temperature via a relatively simple fitting formula designed to approximate Iben's (1982) HR diagram for accreting white dwarfs undergoing steady nuclear burning (see his Figure 2):

$$T \simeq 5.80 \times 10^3 \left[\frac{L}{L_\odot}\right]^{1/4} R_0^{-1/2}(M_{WD}) \left[\frac{L_{crit}}{L_{crit} - L_{nuc}}\right]^{-0.5\alpha(M)} \quad K, \tag{8a}$$

$$R_0(M_{WD}) = \frac{0.0066 \exp(-0.4\, M_{WD})}{(M_{WD} - 0.635)} \tag{8b}$$

$$\alpha(M_{WD}) = 1 - 0.83\,(M_{WD} - 0.7) \quad , \tag{8c}$$

where L_{crit} is obtained by combining equations (4) and (7), and M_{WD} is expressed in solar

units. (The validity of eq. [8b] breaks down for white dwarf masses below ~0.66 $M_\odot$; for such masses the steady burning models of Iben [1982] indicate photospheric radii that become quite large and concomitant effective temperatures that become too low to be of interest in the present study. We therefore eliminated all systems with $M_{WD} < 0.66\ M_\odot$.) We find typical effective temperatures of about 0.5 - 5 × 10^5 K for systems just commencing nuclear burning (Fig. 1d), and 1 - 6 × 10^5 K for systems observed at the current epoch (Fig. 2d).

3.2 "Successful" Supersoft Systems at the Present Epoch

To compute distributions of some of the important observable properties of the supersoft sources, we have utilized calculations such as those illustrated above, but with a significant modification. Systems are weighted according to their lifetimes, with the shorter-lived systems having a smaller probability of existing in the supersoft state at the current epoch. The effective contribution, N, of each successful simulated supersoft system to active systems at the current epoch is taken to be

$$N \simeq \mathcal{R}\,\tau_{KH}/N_{prim} \quad , \tag{9}$$

where $\mathcal{R}$ is the rate of formation of primordial binaries with a primary mass in the range 1.8 – 8 $M_\odot$, τ_{KH} is the Kelvin-Helmholtz time scale of the secondary in that system, and N_{prim} is the number of primordial binaries at the start of the simulations.

Normalized distributions of M_{WD}, M_s, P_{orb}, and T for the Standard Model are shown in Figure 3. They are normalized so that the integral under the distribution equals the number of supersoft systems that should be present in the Galaxy today. The orbital period distribution (for the standard model) indicates a well-defined range of periods for the supersoft systems from 8 hours to 1.4 days (95% confidence), with a median period of 15 hours. The upper limit of ~1.4 days to the orbital period distribution results largely from the fact that stars which fill their Roche lobes in longer period systems are either more massive or have evolved cores. In either case, the lifetimes are relatively shorter and/or the implied mass transfer rates are in excess of $\dot{M}_{crit}$. The two supersoft systems for which orbital periods have been reported, CAL 87 and CAL 83, have periods of 10 hours and 1 day, respectively (see the Introduction).

The distribution of white dwarf masses for the Standard Model is shown in Figure 3b. The 95% confidence limits span the range of 0.7 – 1.05 $M_\odot$, with a median mass of ~ 0.83 $M_\odot$. The distribution of donor-star masses is given in Figure 3c, and indicates that a mass range of 1.3 – 2.7 $M_\odot$ covers 95% of the systems. Finally, in Figure 3d the distribution of white dwarf effective temperatures is given. The range of effective temperatures from ~ (1 – 5) × 10^5 K includes 95% of the systems. The median value of the effective temperature is near 2.3

$\times 10^5$ K. Finally, we point out that none of the above confidence limits takes into account observational selection effects which would tend to strongly favor the discovery of systems with higher effective temperatures.

The integral under the distributions in Figure 3 indicates that, if the assumptions of the Standard Model apply, there should be some 1000 supersoft sources in the Galaxy at the present epoch. Scaling in terms of the masses (Allen 1964), one could reasonably infer that the LMC, the SMC, and M31 should have ~120, 15, and 2800 supersoft sources, respectively, at the present time. In spite of the greater distance to such external galaxies, it may be easier to detect supersoft sources in them than it is in the plane of our own Galaxy as long as the galaxies are at relatively high galactic latitude. The space density of supersoft sources, inferred from the calculated total number of these objects in the Galaxy, implies that the nearest source is on the order of a kiloparsec away. Because a hydrogen column density of only $\sim 10^{21}$ cm^{-2} will absorb most of the very soft X-radiation, a greater number of them should be detectable in nearby external galaxies where the column density through our Galaxy is smaller than $\sim 10^{21}$ cm^{-2}. Of course, only those supersoft sources in an external galaxy which are not behind a large column density of matter in that galaxy will be readily detectable.

Finally, we have run a number of cases in which we have systematically explored the effects of a set of different input assumptions. In each of these cases, we have used all of the assumptions of the Standard Model, save for the one whose effect we wanted to explore. Models 2, 3, and 4 explore the effects of choosing different distributions of mass ratio (q). In Model 2 the mass ratio distribution is flat; in Model 3 the secondary mass is chosen from the same initial mass function as the primary, i.e., independent of the primary mass; and in Model 4, which is based on the work of DM, the mass ratio distribution has a Gaussian shape with a centroid at $q = 0.23$ and rms width equal to 0.42. In Model 5 the mass ratio distribution is the same as for the Standard Model, but the orbital period distribution is modeled on the work of DM; it is Gaussian in shape, centered at 180 days. Model 6 is used to explore the effect of ε, the energy efficiency factor for removing the common envelope; in the simulations for Model 6 we chose $\varepsilon = 0.1$, instead of 0.3. Model 7 differs from all of the others in that, even though the parameters were all chosen to be the same as those of the Standard Model, the time evolution of the binary was explicitly considered. After the common envelope phase, the system was followed via an integration scheme that considered both the nuclear evolution of the secondary (see, e.g., Joss & Rappaport 1983; Di Stefano & Rappaport 1993) and orbital angular momentum losses via "magnetic braking" (see, e.g., Mestel 1968; Verbunt & Zwaan 1981). The properties of all of the above models are summarized in Table 2. The predicted orbital period distributions for all of the models (except for the Standard Model where the P_{orb}

distribution has already been displayed in Figure 3) are shown in Figure 4.

The orbital period distribution for Model 2, where the relation between the primary and secondary masses is looser than in the Standard Model, but still correlated, is very similar to that of the Standard Model. There are slightly fewer (by ~7%) overall supersoft sources predicted in Model 2 due, in part, to the fact that a greater fraction of primordial binaries will have secondary masses that are too small to drive a sufficiently high mass transfer rate. The biggest effect of choosing the secondary mass from the same IMF as the primary (Model 3) is to reduce the expected number of supersoft systems by a factor of ~10. This severe reduction is due to the fact that most of the secondaries in this model have a mass which is too small to lead to unstable mass transfer. We believe, however, that this model is quite unrealistic since there seems to be compelling evidence (see, e.g., Garmany et al. 1980) that in binary systems containing massive stars, the mass of the secondary is usually a substantial fraction of the mass of the primary. Perhaps a more realistic distribution of mass ratios, in which the secondary mass is not well correlated with, but not completely independent of, the mass of the primary, is given by the Gaussian shape suggested by DM (see their §7.4.4; Model 6). The orbital period distribution of supersoft systems for Model 6 shown in Figure 3 indicates that ~25% fewer such systems would be produced than in the Standard Model – the reason is the same as that discussed above for Model 3. The effect of utilizing the DM Gaussian distribution of orbital periods (see their §7.3; Model 5) is to slightly enhance the number of expected supersoft systems (by ~15%). This results from the fact that the DM distribution actually yields a slight increase in the number of primordial binaries with initial orbital periods in the correct range (~1.5 – 8 years) to form supersoft systems than is the case for a flat orbital period distribution. Model 4 (with envelope ejection efficiency factor $\varepsilon = 0.1$) yields an integrated number of supersoft sources that is ~50% *larger* than that of the standard model. The reasons for this non-intuitive result are subtle; however, they revolve around slightly different distributions of orbital separation and constituent masses after the common envelope phase. To help understand the differences, a detailed comparison of the fraction of systems surviving various steps in the evolution is made with the Standard Model in Table 1. Model 7, which includes the effects of magnetic braking on the post-common-envelope orbital evolution, yields ~75% more supersoft systems than the Standard Model and is discussed separately below.

The integrals of the distributions for the seven different models are summarized in Table 2. These represent the numbers of expected supersoft systems in the Galaxy at the present epoch according to each of the models.

The effects associated with following the evolution of the system (Model 7) are somewhat more complex than those associated with any of the other variations we have made to the input

physics. The two elements that we have included in our integrations are the stellar evolution of the secondary and magnetic braking. When we follow the stellar evolution of the secondary, we find that more systems are likely to overfill their Roche lobes at the end of the common envelope phase, and to be excluded from further consideration. This is because the nuclear evolution which has occurred from the birth of the zero-age binary through the time when the primary overfilled its Roche lobe, will tend to expand the secondary. Systems that do survive after the common envelope phase are then integrated into the future, with both the stellar expansion of the secondary due to its own further evolution, and magnetic braking being considered in detail. Although there is a good deal of uncertainty about the exact form of the magnetic braking law, there is observational evidence from the study of close binary systems and individual stars, that emission of a magnetically constrained stellar wind can carry angular momentum from the system and affect its development. For the systems that we are considering, the loss of orbital angular momentum tends to shrink the size of the orbit, so that for each system, mass transfer begins at a shorter orbital period, from donors that have a smaller radius, than for the other models we have considered. This means that some systems, which in the other models would undergo only dynamically unstable mass transfer, may now be considered as potential supersoft sources, since the secondary need not expand across the asymptotic giant branch in order to overfill its Roche lobe. In addition to slightly increasing the pool of systems that may evolve into supersoft sources, the main effect of including magnetic braking is on the observational properties of the binaries during the epoch of mass transfer. In particular, the Kelvin-Helmoltz time associated with a secondary of a particular mass at the commencement of mass transfer will be longer than in the other models. Therefore, in order to have a mass transfer rate that is in the right range, the total amount of mass transferred must be larger. Hence, a generally different set of systems, from those found as supersoft systems in the other models, is selected by the restriction on $\dot{M}$ (see equations 4 and 5). In Model 7, successful supersoft systems tend to contain secondaries with higher mass and to have longer orbital periods than in any of the other models. It also turns out that in this model, the potential type-1a supernova rate is also significantly enhanced.

4. Summary and Conclusions

Starting with a large set of primordial binaries, we have simulated the formation and evolution of binary systems in which unstable mass transfer from a donor star to a white dwarf takes place on a time scale governed by the Kelvin-Helmholtz time of the donor star. We find that a significant number of candidates for supersoft sources naturally emerge from these simulations under a broad range of assumptions about the population of primordial binaries and about the efficiency of envelope ejection during the common envelope phase. These supersoft candidates are identified through mass transfer rates onto the white dwarf that are in the narrow range necessary to allow steady nuclear burning of the accreted matter. The computed nuclear burning rates and the radii of the accreting white dwarfs combine quite naturally to produce effective temperatures of $\sim 3 \times 10^5$ K and luminosities of $\sim 10^{37.5}$ ergs s^{-1}. We find that the donor stars in these supersoft systems have masses that range from ~ 1.3 - 2.7 $M_\odot$, and the orbital periods lie between ~ 8 hours and ~ 1.4 days, consistent with the observed properties of CAL 83 and CAL 87. Thus, the properties of these systems, viz, the orbital periods, masses, luminosities, and effective temperatures are highly consistent with the observations of supersoft X-ray sources (Greiner, Hasinger, & Kahabka 1991; Truemper 1993, private communication; Schaeidt, Hasinger, & Truemper 1993; Orio & Ogelman 1993). There are essentially no "adjustable parameters" in the model that need to be tuned in order to produce these results.

Our study of a range of input assumptions gives an indication of the uncertainties in these predictions. For the population study, one of the largest sources of uncertainty is the state of our knowledge of the true distribution of mass ratios. If the secondary masses are essentially independent of the primary masses, then the numbers we predict are approximately an order of magnitude lower than those for any other scenario. Should such a q distribution be more realistic than the other options considered here, Model 7, in which higher mass secondaries are favored for the production of successful supersoft systems, would perhaps be most dramatically affected. It is more difficult to quantify the possible effects of uncertainties regarding the conditions needed in order for matter accreted onto the white dwarf to be steadily burned. In that regard, it is important to note that the numbers quoted above include only those systems which have passed two applications of a set of fairly restrictive criteria for the mass transfer rates, one at the onset of mass transfer and the other at the current epoch. Some of the systems that have been eliminated by those criteria could possibly exhibit characteristics like those of the observed supersoft sources, at least some of the time. On the other hand, we should also point out that some of the basic assumptions made in this work (e.g., that accretion

mediated by a disk does not affect the rates at which stable nuclear burning occurs) might not be valid and could significantly reduce the production efficiency below that which we have found.

We find for most of the models we have considered, that more than ~1000 such systems should currently be active in our Galaxy and in M31. A smaller but still significant number of such systems should exist in the Large Magellanic Cloud (~100) and in the Small Magellanic Cloud (~15). In fact, we expect that most of the supersoft systems in M31 and the Magellanic Clouds will be substantially absorbed by column densities of a few times 10^{21} cm^{-2}, either in the intervening interstellar medium or in matter surrounding the sources.

We briefly address the time variability (by a factor of ~100 in 3 months and a factor of ~20 in two weeks) that has been reported for one of the newly discovered supersoft sources (Schaeidt et al. 1993). There are two natural ways that source variability could arise within the context of the accreting white dwarf model for supersoft sources. First, since these sources are undergoing rapid mass transfer ($>10^{-7}$ $M_\odot$ yr^{-1}), even a small amount of matter escaping from the system, especially in the orbital plane, could temporarily (or even semi-permanently) severely attenuate the very soft X-ray photons. Second, limit cycles for nuclear burning on white dwarfs have been demonstrated for a range of accretion rates (see, e.g., Iben 1982; Sion & Starrfield 1993). The complete cycle, which involves a "boomerang" shaped trajectory in the HR diagram can have a duration in the range of months to years, but with time scales for the rise to the luminous phase of the cycle as short as days. A careful exploration of nuclear burning patterns for mass accretion rates more appropriate to the model for supersoft sources discussed herein would seem to be worth pursuing. In sharp contrast to the LMXB or black hole models, the present model for supersoft sources predicts that they should remain strictly "soft" sources as long as their luminosity remains above ~10^{37} ergs s^{-1}. Only when such systems drop in luminosity by orders of magnitude (to become ordinary CVs) should non-thermal hard X-ray emission become a substantial component of the spectrum (see, e.g., Pringle & Savonije 1978; Patterson & Raymond 1985; Narayan & Popham 1993). By contrast, for the case of an underlying neutron star or black hole, a supersoft source should appear at some point as a normal luminous hard X-ray source when the mass accretion falls through the correct range of values, below the Eddington limit.

Finally, we comment on the issue of whether the accreting white dwarfs considered in this study might be candidates for producing type-Ia supernovae. Using the same type of calculations presented in this work, we computed the Galactic rate of type-Ia supernovae whose progenitors were supersoft X-ray sources (i.e., systems where the carbon/oxygen white dwarf accreted matter until it was driven over the Chandrasekhar limit). We utilized 3

progressively more conservative criteria to decide if the white dwarf mass would actually grow to 1.4 $M_\odot$. In the first, we assumed that any system with $\dot{M} > 4.4 \times 10^{-8}\ M_\odot\ yr^{-1}$ (~1/10 of $\dot{M}_{stable}$ in eqn. [4] with $M_{WD} = 1.4\ M_\odot$) and with $0.5 \times (M_{WD} + M_s) > 1.4\ M_\odot$ would undergo a type-Ia supernova explosion. The second, more conservative, criterion was the same as the first except that we required $\dot{M} > \dot{M}_{stable}$ (eqn. [4] evaluated at $M_{WD} = 1.4\ M_\odot$). A third test required that $\dot{M}_{stable}(t) < \dot{M} < \dot{M}_{crit}(t)$ during the entire accretion process until M_{WD} exceeded 1.4 $M_\odot$. In our Standard Model we find type-Ia supernova rates in the Galaxy of ~0.006 yr^{-1}, 0.003 yr^{-1}, and $8 \times 10^{-5}\ yr^{-1}$, for the three progressively more restrictive criteria, respectively. Interestingly, our Model 7, which includes the effects of magnetic braking on the post-common-envelope evolution, yields a type-Ia supernova rate as high as 0.0014 yr^{-1} for even the most stringent criterion. The first two of these rates for all of the models, as well as the third rate for Model 7, are clearly encouraging and seem worthy of further investigation. More accurate estimates of the rate of type-Ia supernovae that are descendants of supersoft X-ray sources must await a more realistic treatment of the temporal profile of the unstable mass transfer and a better understanding of the conditions under which the white dwarf can retain most of the mass it accretes when $\dot{M}$ does not lie in the range $\dot{M}_{stable}(t) < \dot{M} < \dot{M}_{crit}(t)$.

The authors thank Joannah Smith for assistance with the computations, and Philipp Podsiadlowski, Ed Sion, Jim Truran, and Ed van den Heuvel for very helpful discussions. This work was supported in part by the National Aeronautics and Space Administration under grants NAGW-1545 and NAG5-1983, and by the Science Scholars Fellowship Program at the Bunting Institute under a grant from the Office for Naval Research.

BIBLIOGRAPHY

Abt, H.A. & Levy, S.G. 1976, ApJS, **30**, 273.

Abt, H.A. & Levy, S.G. 1978, ApJS, **36**, 241.

Abt, H.A. & Levy, S.G. 1985, ApJS, **59**, 229.

Abt, H.A. Gomez, A.E., & Levy, S.G. 1990, ApJS, **74**, 551.

Allen, C.W. 1964, *Astrophysical Quantities*, (New York: Oxford University Press).

Callanan, P.J., Machin, G., Naylor, T., & Charles, P.A. 1989, *MNRAS*, **241**, 37.

Casares, C., Charles , P.A., & Naylor, T. 1992, Nature, **355**, 614.

Cowley, A.P., Schmidtke, P.C., Crampton, D., & Hutchings, J.B. 1990, ApJ, **350**, 288.

de Kool, M. 1992, A&A, **261**, 188.

Doxsey, R., et al. 1976, ApJ, **203**, L9.

Duquennoy, A. & Mayor, M. 1991, A&A, **248**, 485 (DM).

Eggleton, P. 1993, private communication.

Giacconi, R. 1975, in *Proceedings of the 7th Texas Symposium on Relativistic Astrophysics*, Ann. N.Y. Acad. Sci., **262**, 312.

Garmany, C.D., Conti, P.S., & Massey, P. 1980, ApJ, **242**, 1063.

Greiner, J., Hasinger, G., & Kahabka, P. 1991, A&A, **246**, L17.

Hertz, P., Grindlay, J.E., & Bailyn, C.D. 1993, ApJ, **410**, L87.

Iben, I. Jr. 1982, ApJ, **259**, 244.

Joss, P.C., Rappaport, S., & Lewis, W. 1987, ApJ, **319**, 180.

Kippenhahn, R., Kohl, K., & Weigert, A. 1967, Zeits. fur Astrophys., **66**, 58.

Kulkarni, S.R. & Narayan, R. 1988, ApJ, **355**, 755.

Kutter, G.S., & Sparks, W.M. 1981, ApJ, **239**, 998.

Kylafis, N.D., & Xilouris, E. 1993, preprint.

Levine, A., Rappaport, S., Putney, A., Corbet, R., & Nagase, F. 1991, ApJ, **381**, 101.

Livio, M., & Soker, N. 1988, ApJ, **329**, 764.

Livio, M., Prialnik, D., & Regev, O. 1989, ApJ, **341**, 299.

Long, K.S., Helfand, D.J., & Grabelsky, D.A. 1981, ApJ, **248**, 925.

Mestel, L. 1968, MNRAS, **138**, 359.

Meyer, F., & Meyer-Hofmeister, E. 1979, A&A, **78**, 167.

Miller, G.E., & Scalo, J.M. 1979, ApJS, **41**, 513.

Narayan, R., & Popham, R. 1993, CfA preprint.

Naylor, T., Callanan, P.J., Machin, G., & Charles, P.A. 1989, IAU Circ. No. 4747.

Nomoto, K. 1982, ApJ, **253**, 798.

Nomoto, K., Nariai, K., & Sugimoto, D. 1979, PASJ, **31**, 287.
Orio, M., & Ogelman, H. 1993, A&A, in press.
Paczynski, B. 1965, Acta. Astr., **15**, 89.
Paczynski, B. 1967, Acta. Astr., **17**, 193.
Paczynski, B. 1970a, Acta. Astr., **20**, 47.
Paczynski, B. 1970b, Acta. Astr., **20**, 287.
Paczynski, B. 1971, ARA&A, **9**, 183.
Paczynski, B. 1976, in *IAU Symposium 73, Structure and Evolution of Close Binary Systems*, ed P. Eggleton, S. Mitton, & J. Whelan (Dordrecht: Reidel), p.75.
Paczynski, B., & Zytkow, A.N. 1978, ApJ, **222**, 604.
Pakull, M.W., Beuermann, K., van der Klis, M., & van Paradijs, J. 1988, A&A, **203**, L27.
Patterson, J. & Raymond, J.C. 1985, ApJ, **292**, 535.
Politano, M.J. 1988, PhD thesis, University of Illinois.
Prialnik, D., Livio, M., Shaviv, G., & Kovetz, A. 1982, ApJ, **257**, 312.
Pringle, J.E. & Savonije, G.J. 1979, MNRAS, **187**, 777.
Pylyser, E.H.P., Savonije, G.J. 1988, A&A, **191**, 57.
Pylyser, E.H.P., Savonije, G.J. 1989, A&A, **208**, 52.
Rappaport, S., Verbunt, F., & Joss, P.C. 1983, ApJ, **275**, 713.
Savonije, G.J. 1983, in Accretion Driven Stellar X-Ray Sources, eds. W.H.G. Lewin & E.P.J. van den Heuvel (Cambridge: Cambridge University Press), p. 343.
Schaeidt, S., Hasinger, G. & Truemper, J. 1993. A&A, **270**, L9.
Sienkiewicz, R. 1980, A&A, **85**, 295.
Sion, E.M., Acierno, M.J., & Tomcszyk, S. 1979, ApJ, **230**, 832.
Sion, E.M., & Starrfield, S.G. 1986, ApJ, **303**, 130.
Sion, E.M., & Starrfield, S.G. 1993, preprint.
Smale, A.P., et al. 1988, *MNRAS*, **233**, 51.
Sparks, W.M., & Stecher, T.P. 1974, ApJ, **188**, 149.
Sunyaev, R., et al. 1992, ApJ, **389**, L75.
Taam, R.E., Bodenheimer, P., & Ostriker, J.P. 1978, ApJ, **222**, 269.
Taam, R.E. 1980a, ApJ, **237**, 142.
Taam, R.E. 1980b, ApJ, **242**, 749.
Tout, C.A., 1991, MNRAS, **250**, 701.
Truemper, J., et al. 1991, Nature, **349**, 579.
Uus, U. 1970, Nauch. Infor., **17**, 32.
van den Heuvel, E.P.J., Bhattacharya, D., Nomoto, K., & Rappaport, S.A. 1992, A&A, **262**, 97.

van Paradijs, J., & McClintock, J.E. 1993, preprint.

Verbunt, F., & Zwaan, C. 1981, A&A, **100**, L7.

Webbink, R. 1979, in *IAU Colloquium 53, White Dwarfs and Variable Degenerate Stars*, eds. H. van Horn and V. Weidemann (Rochester: University of Rochester Press), p.426.

Webbink, R.F. 1985, in *Interacting Binary Stars*, eds. J.E. Pringle and R.A. Wade (Cambridge Univ. Press: Cambridge), p. 39.

Webbink, R. 1992, in *X-Ray Binaries and Recycled Pulsars*, eds. E.P.J. van den Heuvel and S. Rappaport (Dordrecht: Kluwer), p.269.

Table 1

Candidates for Supersoft Systems After Each Stage of Evolution[a]

Test Number	Test	Fraction Surviving	
		Standard Model	Model 6
1	$1.8 < M_p < 8\ M_\odot$	1.00	1.00
2	$M_s > 0.8\ M_\odot$	0.79	0.79
3	$R_{L,p} > R_p$	0.78	0.78
4	$R_{L,p} < R_{max,p}$	0.36	0.36
5	$R_{L,p} > R_{AGB,p}$	0.26	0.26
6	$R_{L,s} > R_s$	0.095	0.042
7	$M_s > M_{WD}$	0.094	0.041
8	$M_{WD} > 0.66\ M_\odot$	0.064	0.035
9	$R_{L,s} < R_{AGB,s}$	0.033	0.025
10	$\dot{M} > \dot{M}^0_{stable}$	0.029	0.018
11	$\dot{M} < \dot{M}^0_{crit}$	0.0048	0.0075
12	$M_{WD} < 1.4\ M_\odot$	0.0042	0.0067
13	$\dot{M} > \dot{M}_{stable}$	0.0012	0.0020
14	$\dot{M} < \dot{M}_{crit}$	0.0012	0.0020

[a] The fraction of systems which survive various tests during the course of the simulations for the Standard Model and Model 6. The tests and most of the symbols are described in detail in the text. The quantities $R_{L,p}$ and $R_{L,s}$ are the Roche lobe radii of the primary and secondary, respectively; $R_{AGB,p}$ and $R_{AGB,s}$ are the radii of stars of mass M_p and M_s, respectively, when they reach the base of the asymptotic giant branch. Tests 13 and 14 differ from tests 10 and 11 in that the latter pertain to the stable nuclear burning criteria just after mass transfer commences, while the former relate to the conditions for stable nuclear burning at the current epoch (i.e., after the white dwarf has grown in mass).

Table 2

Summary of Model Input Parameters[a]

Model	P_{orb} Distr.	M_s Distr[b]	Env. Ejec. Eff. Factor[c]	Magnet. Braking[d]	Supersoft Systems[e]
Standard	Flat	$q^{1/4}$	0.3	no	1000
2	Flat	Flat in q	0.3	no	930
3	Flat	Equation (1)	0.3	no	100
4	Flat	Gaussian[f]	0.3	no	725
5	Gaussian[f]	$q^{1/4}$	0.3	no	1170
6	Flat	$q^{1/4}$	0.1	no	1500
7	Flat	$q^{1/4}$	0.3	yes	1770

(a) For all models the primary mass was chosen from equation (1), but restricted to the range of 1.8 to 8 $M_\odot$. We assume that such stars are produced at a rate of 0.3 yr^{-1} within the Galaxy, and that half of them are in binary systems. For all but one of the models (5) the distribution of initial orbital periods was taken to be constant per logarithmic interval from 0.5 days to 10^6 years.
(b) The quantity q is defined to be the mass ratio M_s/M_p (<1).
(c) The energy efficiency for ejecting the common envelope is defined by equation (2).
(d) Losses of angular momentum due to magnetic braking in the post-common-envelope evolution were taken into account only in Model 7 (see text for details).
(e) The number of supersoft X-ray sources expected in the Galaxy at the current epoch.
(f) Distributions taken from Duquennoy & Mayor (1991) - see their §7.3 and §7.4.4.

Figure Captions

Figure 1: Luminosity vs. (a) white dwarf mass, (b) mass of donor star, (c) orbital period, and (d) effective temperature of simulated systems just after mass transfer commences (Standard Model). Approximately 10^6 initial binaries were used in the simulation. Each dot represents a single supersoft system, without regard to its lifetime.

Figure 2: Luminosity vs. (a) white dwarf mass, (b) mass of donor star, (c) orbital period, and (d) effective temperature of simulated supersoft X-ray sources at the current epoch (Standard Model). Approximately 3×10^6 initial binaries were used in the simulation. Each dot represents a single supersoft system, without regard to its lifetime.

Figure 3: Distribution of (a) orbital period, (b) white dwarf mass, (c) mass of donor star, and (d) effective temperature for simulated supersoft X-ray sources in the Galaxy at the current epoch (Standard Model). Approximately 3×10^6 initial binaries were used in this simulation. The distributions are normalized to a Galactic production rate of 0.3 stars yr^{-1} in the mass range 1.8 - 8 $M_\odot$.

Figure 4: Orbital period distributions for simulated supersoft systems in the Galaxy at the current epoch. Each panel represents a different model whose input parameters are given in Table 2. Approximately 3×10^6 initial binaries were used in this simulation. The distributions are normalized to a Galactic production rate of 0.3 stars yr^{-1} in the mass range 1.8 - 8 $M_\odot$.

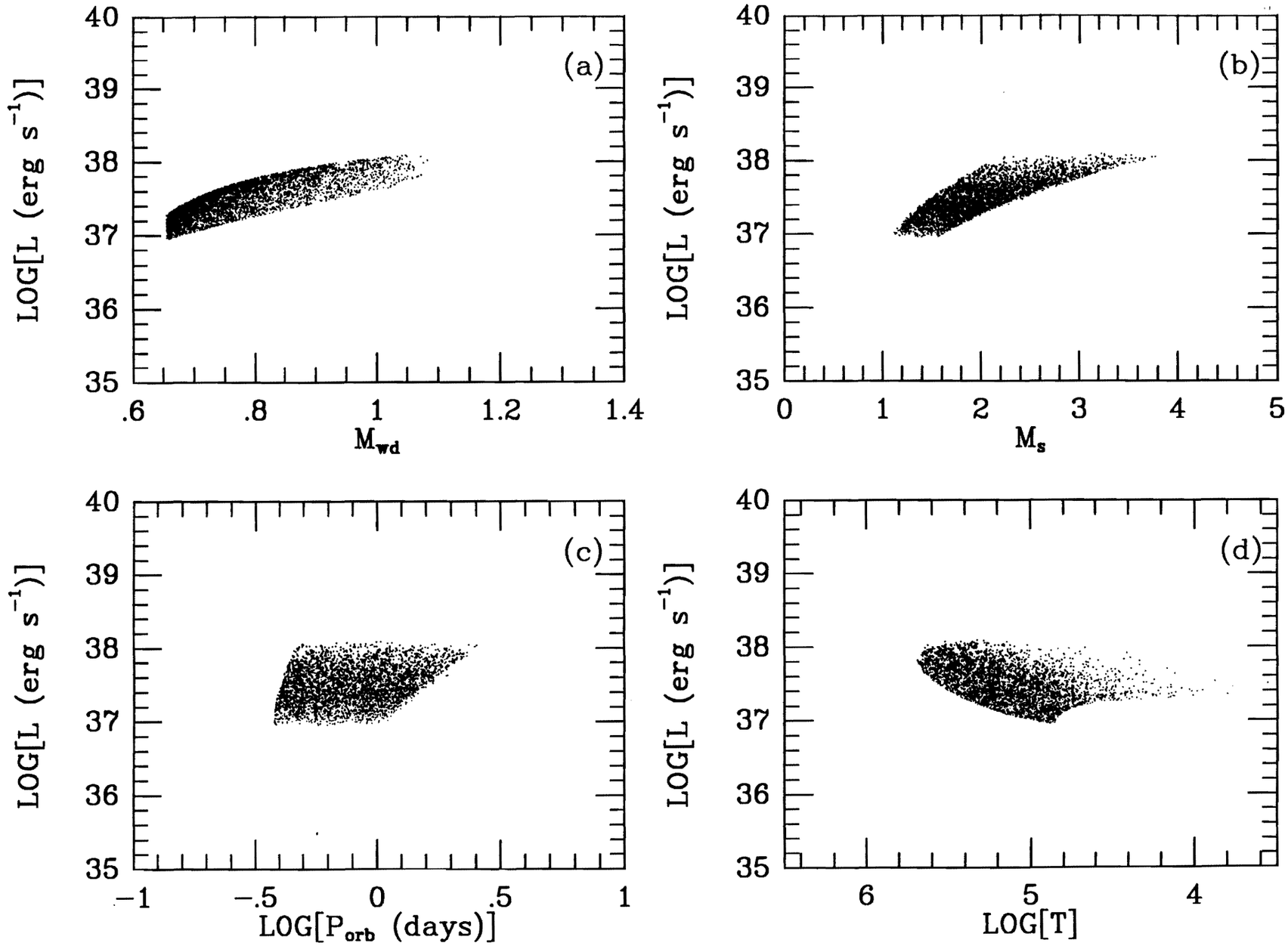
(a)
(b)
(c)
(d)
LOG[L (erg s^{-1})]
M_{wd}
M_s
LOG[P_{orb} (days)]
LOG[T]
40
39
38
37
36
35
.6
.8
1
1.2
1.4
0
2
3
4
5
−1
−.5
.5
6

Figure 1

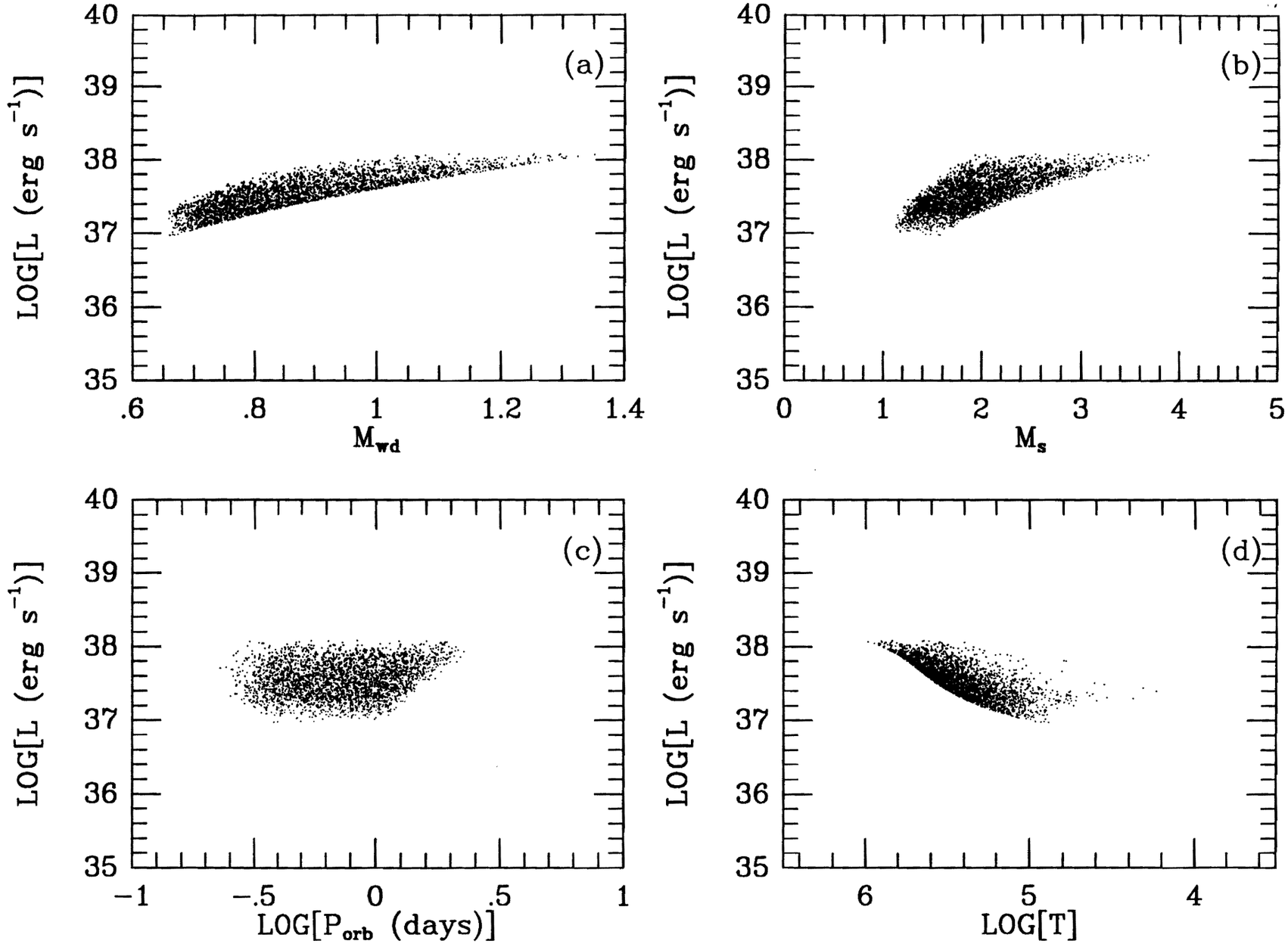
(a)
(b)
(c)
(d)
LOG[L (erg s^{-1})]
M_{wd}
M_s
LOG[P_{orb} (days)]
LOG[T]
40
39
38
37
36
35
.6
.8
1
1.2
1.4
0
2
3
4
5
−1
−.5
.5
6

Figure 2

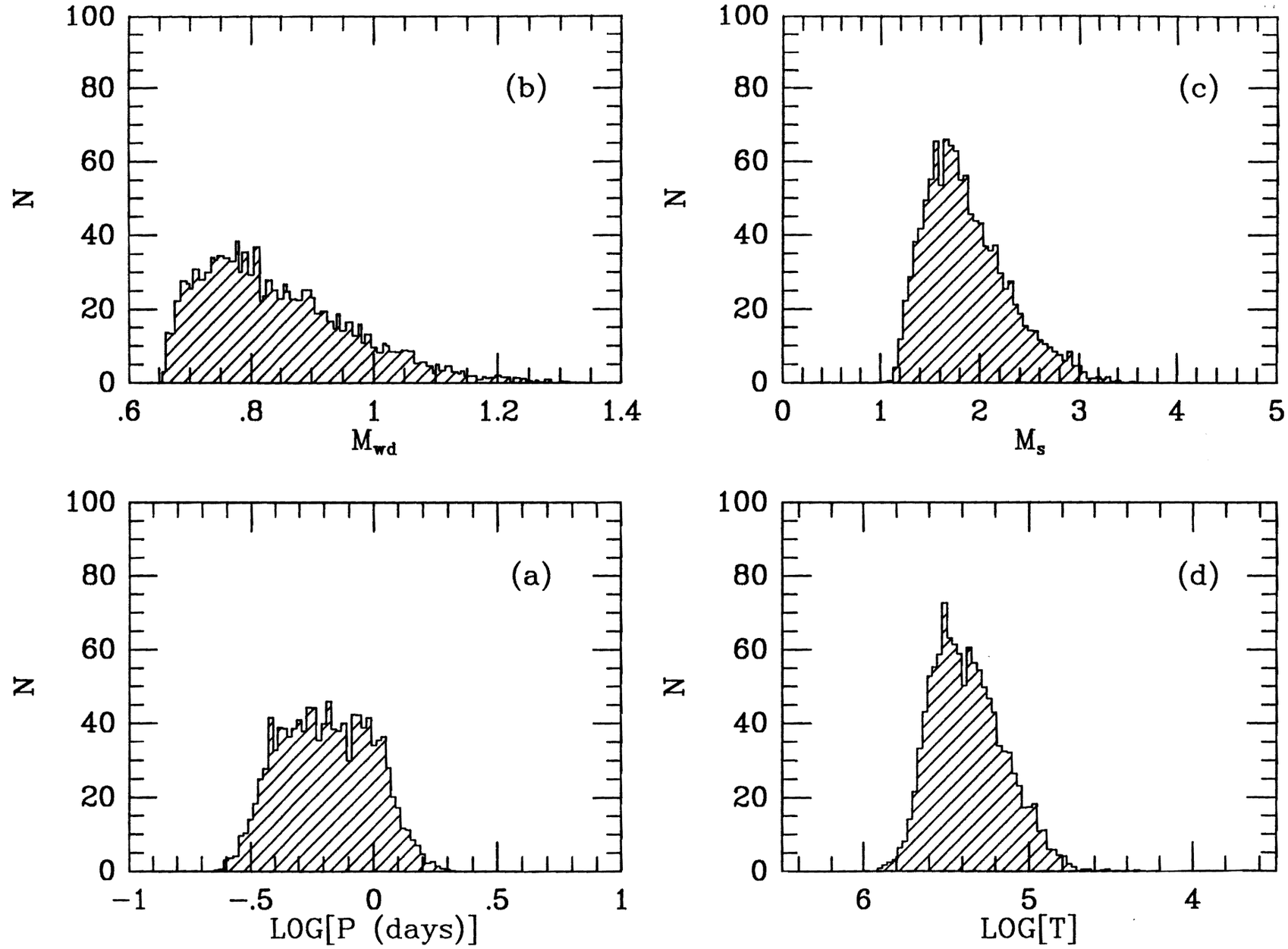

Figure 3

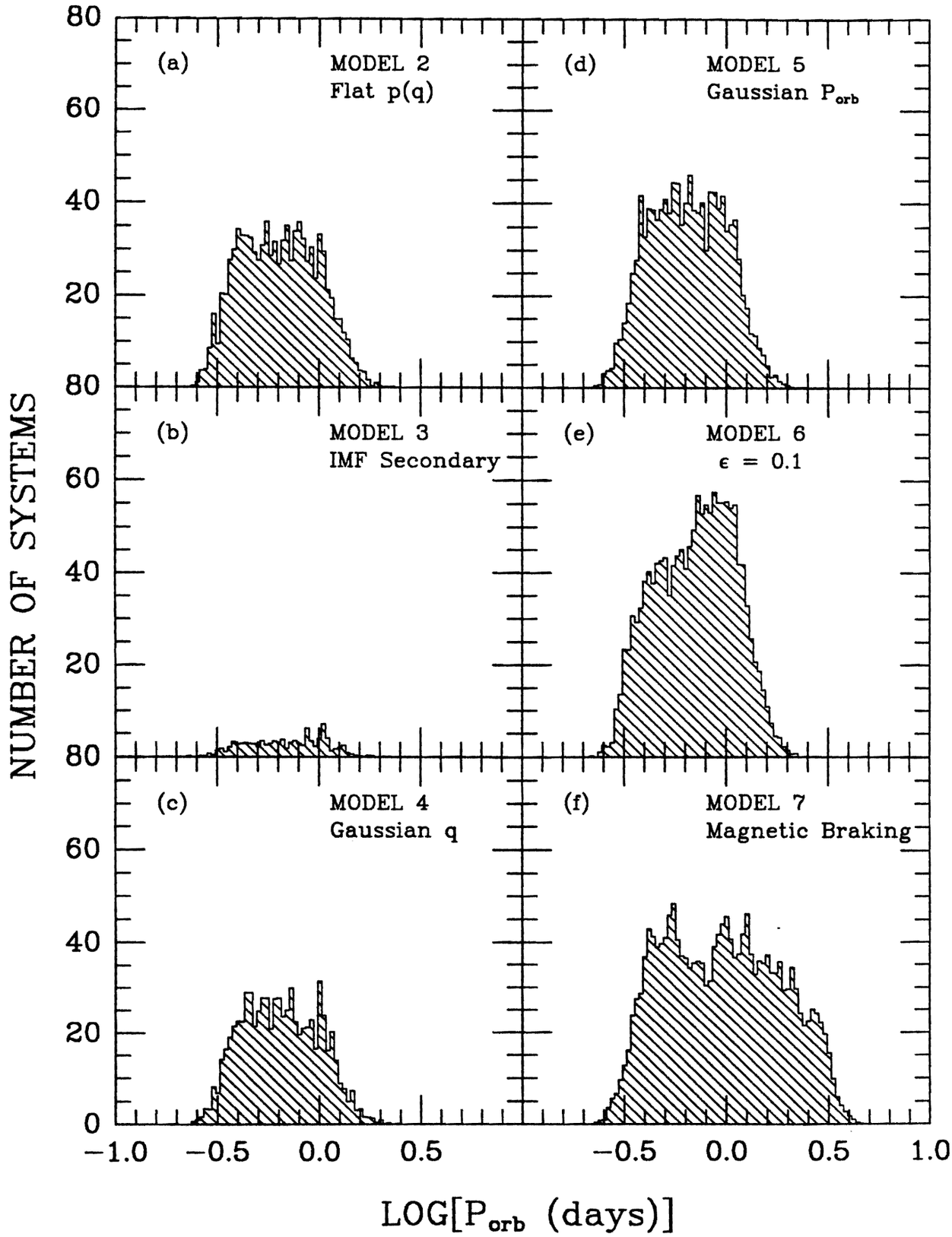
(a)
MODEL 2
Flat p(q)
(b)
MODEL 3
IMF Secondary
(c)
MODEL 4
Gaussian q
(d)
MODEL 5
Gaussian P_{orb}
(e)
MODEL 6
ϵ = 0.1
(f)
MODEL 7
Magnetic Braking
NUMBER OF SYSTEMS
LOG[P_{orb} (days)]
0
20
40
60
80
−1.0
−0.5
0.0
0.5
1.0

Figure 4